EurJOC
European Journal of Organic Chemistry

Communication
doi.org/10.1002/ejoc.202000170

Photochemical Synthesis

Visible-Light-Promoted Efficient Aerobic Dehydrogenation of N-Heterocycles by a Tiny Organic Semiconductor Under Ambient Conditions

Kunyi Yu,[a] Hanjie Zhang,[a] Chenliang Su,*[b] and Yongfa Zhu*[a]

Abstract: An efficient reusable catalytic system has been developed based on perylene diimide (PDI) organic semiconductor for the aerobic dehydrogenation of N-heterocycles with visible light. This practical catalytic system without any additives proceeds under ambient conditions. The minute aggregates of PDI molecules on the surface of SiO_2 nanospheres form tiny organic semiconductors, resulting in high-efficiency photo-oxidative activity. Notably, the robustness of this method is demonstrated by the synthesis of a wide range of N-heteroarenes, gram-scale experiments as well as reusability tests.

N-Heteroarenes are considered privileged structure in nature products, medicinal chemistry and material science.[1] Therefore, the development of mild methods for synthesis of N-heteroarenes has attracted the interest of organic synthetic chemists.[2] The site-selective introduction of substituents onto N-heteroarenes is a formidable challenge, while this is relatively straightforward to achieve for the corresponding N-heterocycles. For example, tetrahydroquinoline can easily undergo 6-site electrophilic substitution functionalization, and the corresponding substituted quinoline can be obtained by dehydrogenation.[3] Therefore, the dehydrogenation of N-heterocycles to N-heteroarenes is considered a viable method.

When compared to thermally promoted organic reaction, the utilization of visible-light energy as a driving force for organic transformation is appealing, as it is a mild, safe, and easy-to-handle energy resource.[4] In general, there are two subclasses of visible-light-promoted dehydrogenation of N-heterocycles: acceptorless[2e,5] and acceptor assisted,[3,6] depending on whether hydrogen acceptors are involved. Acceptor assisted dehydrogenation, especially aerobic oxidative dehydrogenation using oxygen as a cheap and readily available oxidant, has the advantages of scalability and operational simplicity. From the point of view of sustainable development, heterogeneous catalysts are preferable due to facile product separation, catalyst reusability.[2k] In recent years, semiconductor photocatalysis with heterogeneous advantages has been widely used in photocatalytic splitting water into H_2 and O_2, the degradation of organic pollutants and organic synthesis.[7] To the best of our knowledge, only two cases of aerobic dehydrogenation of N-heterocycles by semiconductors have been reported. Operation temperatures up to 80 °C and pure oxygen was required in the mpg-C_3N_4 catalytic system;[8] TEMPO as a co-catalyst was required in the TiO_2 catalytic system.[9] Therefore, an efficient semiconductor photocatalytic protocol that functions under ambient conditions is highly desired.

Perylene diimide (PDI) has been widely used as a basic structural unit for fabricating organic photo-functional materials in recent years due to its unique optical and electronic properties.[10] Compared to some semiconductor photocatalysts (TiO_2 and C_3N_4), easy chemically modified PDIs can be used as functional photocatalysts in various photo-promoted chemical transformation. In 2014, König et al. reported a monomolecular PDI-AN, which can reductively cleave inert C–X bond due to accumulating the energy of two photons.[11] In 2016, Duan et al. reported a metal-organic framework Zn–PDI, which can achieve the photo-oxidation of benzyl alcohol and benzylamine.[12] In the same year, our group reported a self-assembled supramolecule PDINH, capable of photo-oxidative degradation of organic pollutants.[13] In 2017, Chen et al. reported a covalent immobilized PDI-SN, which could be used for photoreductive degradation of halogenated organic pollutants.[14] PDIs exhibit a variety of attractive photocatalytic activities in various phase states, prompting us to develop a new photocatalytic system based on PDI for the photocatalytic aerobic dehydrogenation of N-heterocycles.

Firstly, we examined three heterogeneous photocatalysts based on PDI (Figure 1): PDINH (self-assembly supramolecular), PDI-SN (covalent immobilized to SiO_2 nanospheres) and PDI-U[15] (polymerization with urea) in the aerobic dehydrogenation of N-heterocyclic amines under ambient conditions (see Figure

[a] *Department of Chemistry, Tsinghua University, Beijing 100084, PR China*
E-mail: zhuyf@tsinghua.edu.cn
http://www.zhuyfgroup.com
[b] *International Collaborative Laboratory of 2D Materials for Optoelectronics Science and Technology of Ministry of Education, Engineering Technology Research Center for 2D Materials Information Functional Devices and Systems of Guangdong Province, Institute of Microscale Optoelectronics, Shenzhen University, Shenzhen 518060, PR China*
E-mail: chmsuc@szu.edu.cn
http://2dchem.szu.edu.cn/
Supporting information and ORCID(s) from the author(s) for this article are available on the WWW under https://doi.org/10.1002/ejoc.202000170.

Communication
doi.org/10.1002/ejoc.202000170

S1, b in the Supporting Information), utilizing tetrahydroquinoline (THQ) as the model substrate. To our delight, good catalytic activity was exhibited by all three catalysts (Table 1, entries 1–3). The heterogeneous catalysts remained stable following the catalytic process, apart from supramolecular PDINH, which was structurally destroyed. In particular, the highest photo-oxidative activity was exhibited by PDI-SN, which had a larger specific surface area than PDI-U (27.7 m^2/g for PDI-SN and 12.1 m^2/g for PDI-U). Interestingly, the free monomer PDI-AN (condensation of PDI with 2,6-diisopropyl aniline as showed in Figure 1) did not display any photo-oxidative activity (Table 1, entry 4); the significant differences in catalytic activity between the free monomer PDI-AN and PDI-SN prompted us to examine the phase state of the PDI molecules in PDI-SN. Compared with the free monomer PDI-AN, the wide peak in the UV/Vis absorption spectrum of PDI-SN implied that the PDI molecules exist in aggregation state in PDI-SN (see Figure S8 in the Supporting Information). In addition, the fluorescence emission spectra of the supramolecular PDINH and PDI-SN supported the hypothesis mentioned above (see Figure S8 in the Supporting Information). Unlike the thick layer of the polymer PDI-U semiconductors, PDI-SN consists of minute aggregates of PDI molecules on the surface of SiO_2 nanospheres, which form thin layers of PDI semiconductors, resulting in a higher photogenic carrier transport efficiency, and superior photo-oxidative activity. In other words, the particular aggregation of PDI molecules in PDI-SN ensured both photo-oxidative activity and the high catalytic efficiency.

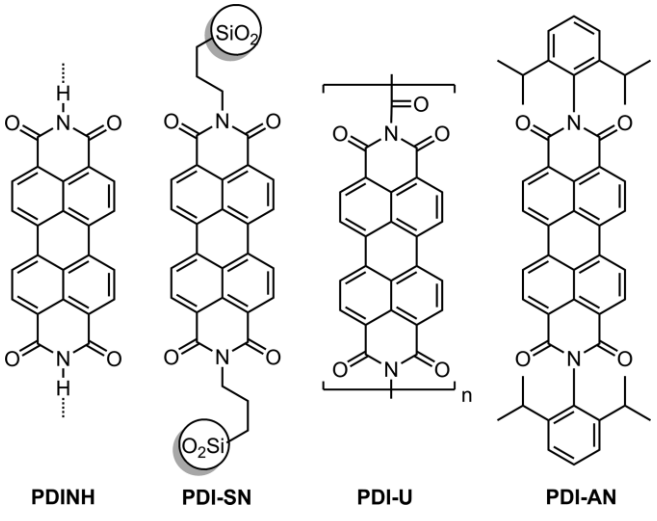

Figure 1. PDIs in different phase states.

Next, we carried out solvent optimization experiments. The current catalyst has catalytic activity in many polar solvents such as DMA, DMF, DMSO, MeCN, and water. However, no product was obtained when using methanol, which probably acted as a role of electron donor and quenched the photo-generated holes (see Table S3 in the Supporting Information). In order to determine the necessity of each component, namely the catalyst, LED irradiation and air, a number of control experiments were conducted, and the results indicated that they were all indispensable components (Table 1, entries 5–7). In addition,

Table 1. Optimization of the reaction conditions.[a,b]

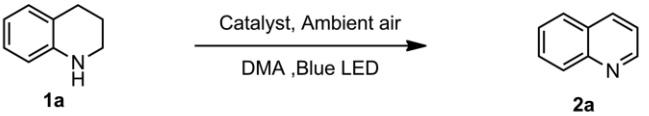

1a 2a

Entry	Catalyst	Yield (%)
1	PDINH	83
2	PDI-U	54
3	PDI-SN	94(91)[c]
4	PDI-AN	trace
5	none	trace
6	PDI-SN	trace[d]
7	PDI-SN	14[e]
8	TiO_2	8
9	C_3N_4	18

[a] Reaction conditions: THQ (**1a**, 0.2 mmol), catalyst (5 mg), DMA (1 mL), ambient air atmosphere under 18 W 400 nm LED irradiation overnight. [b] Yield determined by GC analysis with an internal standard (dodecane). [c] Isolated yield. [d] In the absence of light. [e] Under Ar atmosphere.

wavelengths of LED light sources were studied, with 400 nm leading to the highest catalytic activity (see Table S2 in the Supporting Information). Comparatively, the inorganic semiconductors TiO_2 and organic semiconductor bulky g-C_3N_4 exhibited poor activity under standard reaction conditions (Table 1, entries 8–9).

With the optimal reaction conditions in hand, this practical catalytic protocol was then applied to the aerobic dehydrogenation of diverse cyclic amines. As shown in Table 2, various substituted tetrahydroquinolines and indolines were compatible and the expected dehydrogenated products were obtained in good to excellent yields. Tetrahydroquinolines bearing a methyl, substituted at 2-, 3-, 4- and 6- positions were well tolerated; the 2-position substitution afforded slightly lower yields. It is probably due to the higher degree of steric hindrance at the 2-position compared to that at the other positions (Table 2, **2b**–**2e**). A variety of 6-substituted tetrahydroquinolines were successfully subjected to this practical catalytic system; electron-deficient substitutions gave superior results (Table 2, **2f**–**2h**). The readily oxidized phenol, as well as aniline fragments were likewise compatible, thus the 8-substituted hydroxyquinoline and aminoquinoline being produced in 93 % and 88 % yield, respectively (Table 2, **2i**–**2j**). Similarly, various substituted indolines gave the corresponding indoles in good yields (Table 2, **2k**–**2q**), except for 2-indoleic acid (Table 2, **2r**). The ternary heterocyclic dihydroacridine likewise performed successful (Table 2, **2s**). Finally, a heterocyclic substrate containing two nitrogen atoms were investigated and the corresponding quinoxaline was obtained in good yield (Table 2, **2t**).

Encouraged by these results, we attempted to apply this practical catalytic protocol to cyclic amines generated in situ. As shown in Table 3, we investigated a strategy whereby benzylamine was the precursor for the imine; it reacted with *o*-phen-

Communication
doi.org/10.1002/ejoc.202000170

Chemistry Europe
European Chemical Societies Publishing

Table 2. Aerobic dehydrogenation of cyclic amines.[a,b]

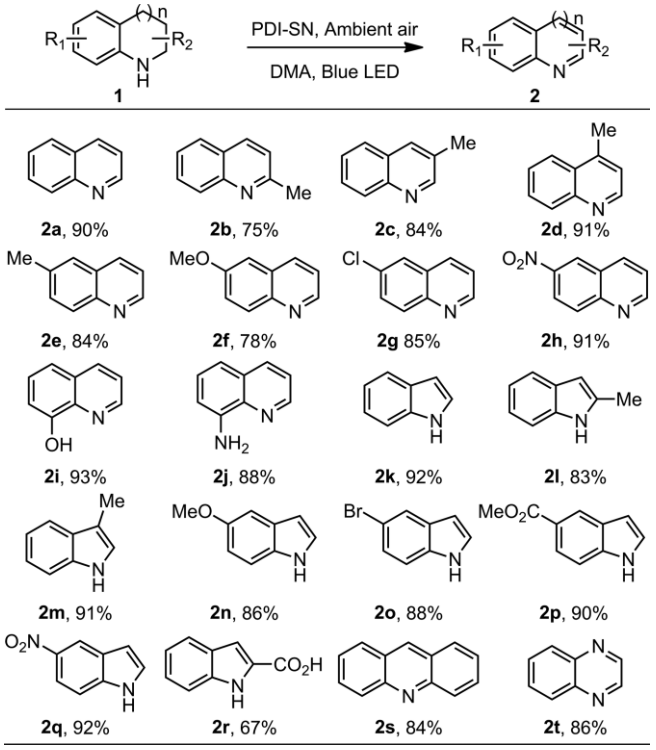

[a] Reaction conditions: cyclic amines (**1**, 0.4 mmol), PDI-SN (10 mg), DMA (2 mL), ambient air atmosphere under 18 W 400 nm LED irradiation overnight. [b] Isolated yield.

ylenediamine to form a cyclic amine intermediate, after which dehydrogenative aromatization afforded 2-phenyl-benzoimidazole (Table 3, **5a**) in an isolated yield of 91 %. Benzylamines with varying electronic properties were compatible, including those substituted with electron-donating group, such as a methoxy (Table 3, **5b**), and electron-withdrawing group, such as nitro group (Table 3, **5c**); the corresponding products were obtained in 87 % and 93 % yield, respectively. In addition, the

Table 3. Aerobic dehydrogenation of cyclic amines generated in situ.[a,b]

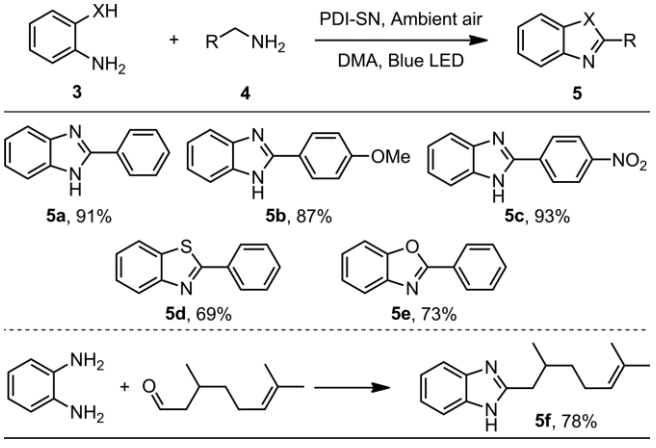

[a] Reaction conditions: *o*-diaminobenzene (**3**, 0.4 mmol), Benzylamine or aldehyde (**4**, 0.44 mmol), PDI-SN (10 mg), and DMA (2 mL), ambient air atmosphere under 18 W 400 nm LED irradiation overnight. [b] Isolated yield.

combinations of *o*-hydroxyaniline and *o*-mercaptoaniline with benzylamines were studied, and the corresponding 2-phenyl-benzoxazole (Table 3, **5d**) and 2-thiophene benzoxazole (Table 3, **5e**) were generated in 69–73 % yield under standard reaction condition. Finally, vanillic aldehyde was not oxidized to vanillic acid in this photo-oxidative system, and the desired product benzimidazole derivative (Table 3, **5f**) was obtained in a yield of 78 %.

As agglomeration of heterogeneous nanocatalysts is ubiquitous deficient,[2k] we examined the reusability of the present catalyst by performing six consecutive experimental runs (see the Supporting Information for details of the recycling procedure). To our delight, no significant reduction (Figure 2) were observed in yield (83–91 %). In addition, no significant changes were seen in the UV and IR spectra of the catalyst isolated by centrifugal filtration, compared with fresh catalyst (see Figure S3 in the Supporting Information).

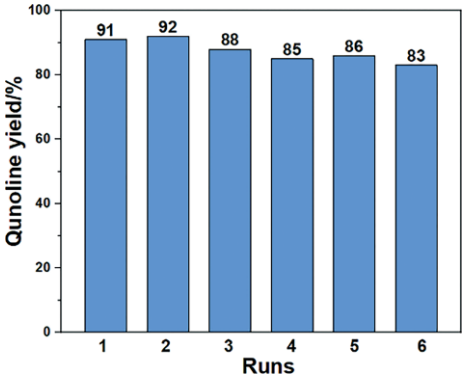

Figure 2. Recycling test of the PDI-SN catalyst. Reaction conditions: THQ (**1a**, 0.4 mmol), PDI-SN (20 mg), DMA (2 mL), ambient air atmosphere under 18 W 400 nm LED irradiation overnight.

To evaluate the scalability of the aerobic dehydrogenation protocol, a gram-scale experiment was performed (see the Supporting Information for details of the gram-scale reaction procedure). We found that the reactivity was no significant altered in this case, and the gram-scale reaction proceeded smoothly, giving the product in an isolated yield of 82 % by a prolonged reaction time of up to 72 h, and with a combination light source (Scheme 1).

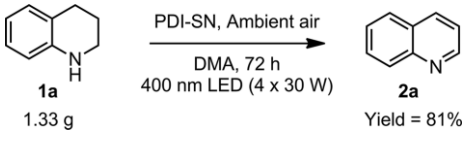

Scheme 1. Gram-scale preparation for the aerobic dehydrogenation of THQ. Reaction conditions: THQ (**1a**, 10 mmol), PDI-SN (500 mg), DMA (50 mL), ambient air atmosphere under 4 × 30 W 400 nm LED irradiation 72 h.

In order to determine the possible intermediates and reaction mechanism, a series of quenching and trapping experiments were performed (Figure 3).[16] The detection of reactive oxygen species was conducted firstly. The reaction proceeded unaffectedly in the presence of TBA,[17] a well-known hydroxyl radical (HO•) quenching agent, which indicated that no HO• was involved. Similarly, the reaction is unaffected by the presence

of singlet oxygen quenching ($^1O_2$) agent DBACO,[18] which indicated that $^1O_2$ was not the reactive oxygen species. In the presence of superoxide radical ($O_2^{\bullet-}$) quenching agent BHT,[19] a significantly reduction in yield suggested that the reaction mechanism entail a $O_2^{\bullet-}$, and analogous results were obtained in nitrotetrazolium blue chloride (NBT) control experiments.[20] The reduction in reactivity in the presence of the photo-generated electron quenching agent AgOTf,[21] likewise supported the existence of $O_2^{\bullet-}$ intermediates. The reaction was severely hampered in the presence of photo-generated holes quenching agent EG.[22] Reduction quenching generally required participation by the photo-generated holes and fluorescence quenching experiments indicated electrons transfer from tetrahydroquinoline to organic semiconductor (see Figure S9 in the Supporting Information). The presence of TEMPO reduced the reaction yield, which supported a free radical pathway.[23] Finally, H_2O_2 as a possible by-product was also detected in a typical horseradish peroxidase experiment.[24]

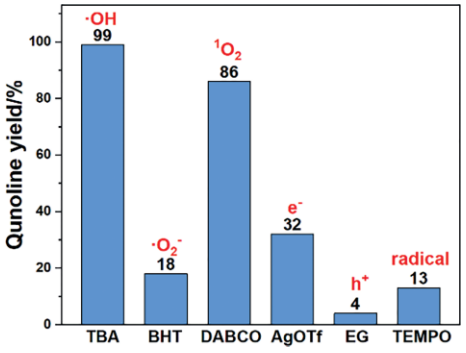

Figure 3. Experimental results of mechanism research. Reaction conditions: THQ (**1a**, 0.2 mmol), quenching agent (0.4 mmol), PDI-SN (5 mg), DMA (1 mL), ambient air atmosphere under 18 W 400 nm LED irradiation overnight. TBA = *tert*-butyl alcohol; BHT = butylated hydroxytoluene; DABCO = bicyclo[2.2.2]-1,4-diazaoctane; AgOTf = silver triflate; EG = ethylene glycol; TEMPO = 2,2,6,6-tetramethylpiperidinyl *N*-oxide radical.

Based on the above experimental results and known literatures,[3,5a,5b,5d,8] we proposed a possible reaction mechanism (Scheme 2). Firstly, oxidative photo-generated holes and reductive photo-generated electrons are produced by excitation of the organic semiconductor PDI-SN, respectively. Then, the substrate **1a** is oxidized by photo-generated holes by single electron transfer (HAT),[25] thereby producing the corresponding cation radical **A**; O_2 from the air is reduced by photo-generated electrons, thereby producing a $O_2^{\bullet-}$, respectively. Coherently, the radical cation **A** is oxidized by $O_2^{\bullet-}$ to form an imine cation intermediate **B**, via the so-called hydrogen-atom transfer (HAT) mechanism.[3] Consequently, Imine intermediate **C** is obtained from the imine cation **B** by the release of one proton (H^+) with a concomitant generation of H_2O_2. The imine **C** can be rapidly isomerized to intermediate **D**.[5a,26] The second dehydrogenation step could be completed by another catalytic cycle or aromatization,[3,5a] providing the final dehydrogenation product **2a**.

In summary, we have reported an efficient semiconductor photocatalytic system for the aerobic dehydrogenation of N-heterocycle under ambient conditions. This reusable photo-

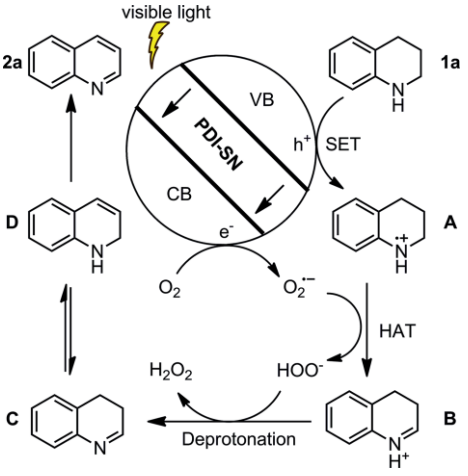

Scheme 2. Proposed mechanism for the aerobic dehydrogenation of THQ.

catalytic system proceeds under very mild conditions: in the ambient air atmosphere, without additional heat sources and additives. The minute aggregates of PDI molecules on the surface of SiO_2 nanospheres form tiny PDI semiconductors, resulting in high-efficiency photo-oxidative activity. This practical catalytic protocol is attractive, and offers a wide scope related to the synthesis of quinoline, indole, benzimidazole, benzothiazole and benzoxazole derivatives. The mechanistic studies show that photo-generated holes and $O_2^{\bullet-}$ are pivotal components in the reaction pathway.

Conflict of Interest

The authors declare no conflict of interest.

Acknowledgments

This work was partly supported by the Chinese National Science Foundation (21437003, 21673126, 21761142017, 21621003, and 21972094), the Beijing Municipal Science and Technology Project (Z181100005118007), the Collaborative Innovation Center for Regional Environmental Quality, the Shenzhen Peacock Plan (KQJSCX20170727100802505 and KQTD2016053112042971), the Guangdong Special Support Program, and the Pengcheng Scholar program. The authors thank Dr. Chuntian Qiu, Shenzhen University, for providing important advice in preparing manuscripts.

Keywords: Aerobic dehydrogenation · Nitrogen heterocycles · Perylene diimide · Organic semiconductors · Photocatalysis

[1] O. Afzal, S. Kumar, M. R. Haider, M. R. Ali, R. Kumar, M. Jaggi, S. Bawa, *Eur. J. Med. Chem.* **2015**, *97*, 871–910.
[2] a) S. Chakraborty, W. W. Brennessel, W. D. Jones, *J. Am. Chem. Soc.* **2014**, *136*, 8564–8567; b) A. E. Wendlandt, S. S. Stahl, *J. Am. Chem. Soc.* **2014**, *136*, 11910–11913; c) A. E. Wendlandt, S. S. Stahl, *J. Am. Chem. Soc.* **2014**, *136*, 506–512; d) X. Cui, Y. Li, S. Bachmann, M. Scalone, A. E. Surkus, K. Junge, C. Topf, M. Beller, *J. Am. Chem. Soc.* **2015**, *137*, 10652–10658; e) S. Chen, Q. Wan, A. K. Badu-Tawiah, *Angew. Chem. Int. Ed.* **2016**, *55*, 9345–9349; *Angew. Chem.* **2016**, *128*, 9491–9495; f) D. Forberg, T. Schwob, M. Zaheer, M. Friedrich, N. Miyajima, R. Kempe, *Nat. Commun.* **2016**, *7*,

13201; g) D. Jung, M. H. Kim, J. Kim, *Org. Lett.* **2016**, *18*, 6300–6303; h) M. Kojima, M. Kanai, *Angew. Chem. Int. Ed.* **2016**, *55*, 12224–12227; *Angew. Chem.* **2016**, *128*, 12412–12415; i) Y. Han, Z. Wang, R. Xu, W. Zhang, W. Chen, L. Zheng, J. Zhang, J. Luo, K. Wu, Y. Zhu, C. Chen, Q. Peng, Q. Liu, P. Hu, D. Wang, Y. Li, *Angew. Chem. Int. Ed.* **2018**, *57*, 11262–11266; *Angew. Chem.* **2018**, *130*, 11432–11436; j) D. Xu, H. Zhao, Z. Dong, J. Ma, *ChemCatChem* **2019**, *11*, 5475–5486; k) X. Bi, T. Tang, X. Meng, M. Gou, X. Liu, P. Zhao, *Catal. Sci. Technol.* **2020**, *10*, 360–371.

[3] M. K. Sahoo, G. Jaiswal, J. Rana, E. Balaraman, *Chem. Eur. J.* **2017**, *23*, 14167–14172.

[4] a) X. Li, J. Yu, M. Jaroniec, *Chem. Soc. Rev.* **2016**, *45*, 2603–2636; b) S. Lazzaroni, D. Ravelli, S. Protti, M. Fagnoni, A. Albini, *C. R. Chim.* **2017**, *20*, 261–271.

[5] For selected examples on the visible-light-promoted acceptorless dehydrogenation of N-heterocycles, see: a) K. H. He, F. F. Tan, C. Z. Zhou, G. J. Zhou, X. L. Yang, Y. Li, *Angew. Chem. Int. Ed.* **2017**, *56*, 3080–3084; *Angew. Chem.* **2017**, *129*, 3126–3130; b) M. Zheng, J. Shi, T. Yuan, X. Wang, *Angew. Chem. Int. Ed.* **2018**, *57*, 5487–5491; *Angew. Chem.* **2018**, *130*, 5585–5589; c) M. Hao, X. Deng, L. Xu, Z. Li, *Appl. Catal. B* **2019**, *252*, 18–23; d) M. K. Sahoo, E. Balaraman, *Green Chem.* **2019**, *21*, 2119–2128.

[6] For selected examples on the visible-light-promoted acceptor assisted dehydrogenation of N-heterocycles, see: a) K. Suzuki, F. Tang, Y. Kikukawa, K. Yamaguchi, N. Mizuno, *Angew. Chem. Int. Ed.* **2014**, *53*, 5356–5360; *Angew. Chem.* **2014**, *126*, 5460–5464; b) T. Shao, Y. Yin, R. Lee, X. Zhao, G. Chai, Z. Jiang, *Adv. Synth. Catal.* **2018**, *360*, 1754–1760.

[7] Recent reviews on semiconductor photocatalysis, see: a) N. Serpone, A. V. Emeline, *J. Phys. Chem. Lett.* **2012**, *3*, 673–677; b) S. Perathoner, C. Ampelli, S. Chen, R. Passalacqua, D. Su, G. Centi, *J. Energy Chem.* **2017**, *26*, 207–218; c) A. Savateev, I. Ghosh, B. König, M. Antonietti, *Angew. Chem. Int. Ed.* **2018**, *57*, 15936–15947; *Angew. Chem.* **2018**, *130*, 16164–16176; d) I. Ghosh, J. Khamrai, A. Savateev, N. Shlapakov, M. Antonietti, B. König, *Science* **2019**, *365*, 360–366.

[8] F. Su, S. C. Mathew, L. Mohlmann, M. Antonietti, X. Wang, S. Blechert, *Angew. Chem. Int. Ed.* **2011**, *50*, 657–660; *Angew. Chem.* **2011**, *123*, 683–686.

[9] For selected examples on PDI fabricating organic photo-functional materials, see: a) D. Görl, X. Zhang, F. Werthner, *Angew. Chem. Int. Ed.* **2012**, *51*, 6328–6348; *Angew. Chem.* **2012**, *124*, 6434–6455; b) D. Schmidt, M. Son, J. M. Lim, M.-J. Lin, I. Krummenacher, H. Braunschweig, D. Kim, F. Werthner, *Angew. Chem. Int. Ed.* **2015**, *54*, 13980–13984; *Angew. Chem.* **2015**, *127*, 14186–14190; c) P. Spenst, F. Werthner, *Angew. Chem. Int. Ed.* **2015**, *54*, 10165–10168; *Angew. Chem.* **2015**, *127*, 10303–10306; d) A. H. Endres, M. Schaffroth, F. Paulus, H. Reiss, H. Wadepohl, F. Rominger, R. Krämer, U. H. F. Bunz, *J. Am. Chem. Soc.* **2016**, *138*, 1792–1795; e) D. Meng, D. Sun, C. Zhong, T. Liu, B. Fan, L. Huo, Y. Li, W. Jiang, H. Choi, T. Kim, J. Y. Kim, Y. Sun, Z. Wang, A. J. Heeger, *J. Am. Chem. Soc.* **2016**, *138*, 375–380; f) A. Zhang, C. Li, F. Yang, J. Zhang, Z. Wang, Z. Wei, W. Li, *Angew. Chem. Int. Ed.* **2017**, *56*, 2694–2698; *Angew. Chem.* **2017**, *129*, 2738–2742.

[10] N. O. Balayeva, N. Zheng, R. Dillert, D. W. Bahnemann, *ACS Catal.* **2019**, *9*, 10694–10704.

[11] I. Ghosh, T. Ghosh, J. I. Bardagi, B. König, *Science* **2014**, *346*, 725–728.

[12] L. Zeng, T. Liu, C. He, D. Shi, F. Zhang, C. Duan, *J. Am. Chem. Soc.* **2016**, *138*, 3958–3961.

[13] D. Liu, J. Wang, X. Bai, R. Zong, Y. Zhu, *Adv. Mater.* **2016**, *28*, 7284–7290.

[14] J. Shang, H. Tang, H. Ji, W. Ma, C. Chen, J. Zhao, *Chin. J. Catal.* **2017**, *38*, 2094–2101.

[15] P. Sharma, D. Damien, K. Nagarajan, M. M. Shaijumon, M. Hariharan, *J. Phys. Chem. Lett.* **2013**, *4*, 3192–3197.

[16] For detailed information, see the Supporting Information.

[17] H. Che, C. Liu, W. Hu, H. Hu, J. Li, J. Dou, W. Shi, C. Li, H. Dong, *Catal. Sci. Technol.* **2018**, *8*, 622–631.

[18] M. Klaper, T. Linker, *J. Am. Chem. Soc.* **2015**, *137*, 13744–13747.

[19] F. Su, S. C. Mathew, G. Lipner, X. Fu, M. Antonietti, S. Blechert, X. Wang, *J. Am. Chem. Soc.* **2010**, *132*, 16299–16301.

[20] A. M. Czoska, S. Livraghi, M. Chiesa, E. Giamello, S. Agnoli, G. Granozzi, E. Finazzi, C. D. Valentin, G. Pacchioni, *J. Phys. Chem. C* **2008**, *112*, 8951–8956.

[21] J. Zhang, Y. Hu, J. Qin, Z. Yang, M. Fu, *Chem. Eng. J.* **2020**, *385*, 123814.

[22] R. A. Geioushy, S. M. El-Sheikh, A. B. Azzam, B. A. Salah, F. M. Eldars, *J. Hazard. Mater.* **2020**, *381*, 120955.

[23] D. R. Chambers, A. Juneau, C. T. Ludwig, M. Frenette, D. B. C. Martin, *Organometallics* **2019**, *38*, 4570–4577.

[24] A. M. Azevedo, V. C. Martins, D. M. F. Prazeres, V. Vojinović, J. M. S. Cabral, L. P. Fonseca, *Biotechnol. Annu. Rev.* **2003**, *9*, 199–247.

[25] The results of Stern-Volmer luminescence quenching experiment can support the single electron transfer (SET) from tetrahydroquinoline to photo-induced holes (see supporting information).

[26] H. Li, J. Jiang, G. Lu, F. Huang, Z. Wang, *Organometallics* **2011**, *30*, 3131–3141.

Received: February 6, 2020